Title

Variational Theory of the Radiant Emittance of the Mercury Argon Discharge and the Effects of Isotopic Enrichment

Authors

Richardson, R.W.
Berman, S.M.

Publication Date

1991

LBL-31020 Rev.
UC-427
Preprint

Lawrence Berkeley Laboratory

UNIVERSITY OF CALIFORNIA

ENERGY & ENVIRONMENT DIVISION

Submitted to Journal of Applied Physics

Variational Theory of the Radiant Emittance of the Mercury Argon Discharge and the Effects of Isotopic Enrichment

R.W. Richardson and S.M. Berman

January 1991

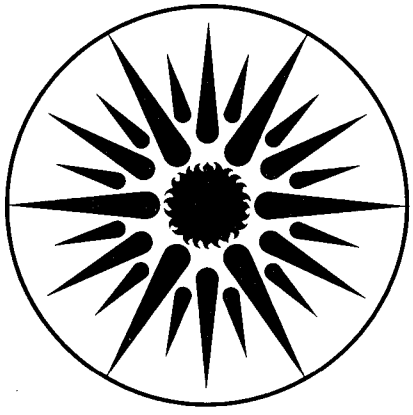

ENERGY & ENVIRONMENT DIVISION

Prepared for the U.S. Department of Energy under Contract Number DE-AC03-76SF00098

DISCLAIMER

L-156
LBL-31020 Rev.

VARIATIONAL THEORY OF THE RADIANT EMITTANCE OF THE MERCURY ARGON DISCHARGE AND THE EFFECTS OF ISOTOPIC ENRICHMENT

R.W. Richardson[1] and S.M. Berman

Lighting Systems Research Group
Energy & Environment Division
Lawrence Berkeley Laboratory
Berkeley, California 94720

[1]Permanent Address:

Physics Department
New York University
4 Washington Place
New York, New York 10003

January 1991

This work was supported by the Assistant Secretary for Conservation and Renewable Energy, Office of Building Technologies, Building Equipment Division of the U.S. Department of Energy under Contract No. DE-AC03-76SF00098.

VARIATIONAL THEORY OF THE RADIANT EMITTANCE OF THE MERCURY ARGON DISCHARGE AND THE EFFECTS OF ISOTOPIC ENRICHMENT

ABSTRACT

A Variational theory of the radiant emittance of the Mercury-Argon discharge is developed and applied to an investigation of the effects of alterations of the isotopic composition of the Mercury. The theory includes the effects of transport of resonance radiation, elastic and inelastic collisions, resonant exchange of excitation, diffusion of the Mercury atoms, the isotope- and hyperfine-shifted structure of the resonance line, and the surfaces of the discharge on the emittance. Two sensitive parameters - the branching ratio for radiative decay of the resonance state and the rate constant for resonant exchange of excitation - are fitted to data on natural Mercury. The remaining insensitive parameters are given values based on microscopic estimates. The resulting theory reproduces the experimentally observed results for Mercury - 196 enhanced mixtures. We predict small effects for mixtures with other isotopes enhanced. The crucial role played by resonant exchange of excitation is emphasized.

1. Introduction.

The Mercury-Argon discharge is a system with both fundamental and practical applications. From the fundamental point of view, it has been used to measure atomic properties such as inelastic collision cross sections and has been a laboratory for radiation transport studies. From the practical point of view, it is the basis of fluorescent lighting technology which makes use of it as an efficient device for converting electrical energy into ultra violet radiation which is subsequently converted into visible light by phosphors on the inner surface of the tube. Small improvements in the efficiency of such devices can lead to major savings of energy. The property of the discharge that is of primary interest in evaluating its effectiveness as a light source is its radiant emittance or the flux of UV radiation at the surface of the discharge. In this paper, we develop a variational theory of this emittance and apply it to an assessment of the effects of isotopic enrichment of the Mercury.

The modern theory of resonance radiation transport in discharges begins with the works of Biberman[1] and Holstein[2]. They developed an integrodifferential equation for the density of excited state atoms as a function of time and position in the discharge. We review and extend this equation in Sec. 2 for time independent situations. The extensions that we give include allowance for the effects of diffusion of the excited state atoms and the influence of the surface of the discharge, elastic and inelastic collisions, collisional transfer of excitation between

the Mercury atoms, and the ten components of the isotope- and hyperfine-shifted 254 nm $^3P_1 \rightarrow {}^1S_0$ resonance line of Mercury. While we determine the excited state densities variationaly, they can be obtained empirically from the angular distribution of the resonance radiation at the surface of the discharge using the analytical inversion of the generalized Abel equation[3] that gives this angular distribution in terms of a radially varying source density for an optically thick discharge.

The diffusion of the excited state atoms is important as it allows one to impose the appropriate boundary conditions on their densities at the surface of the discharge. The radiant emittance of an optically thick discharge is sensitive to the behavior of these densities at the surface. We use a destroying boundary condition derived from the kinetic picture that all excited state atoms incident upon the surface are deexcited at the surface and there is no return current of excited atoms into the discharge from the surface. This leads to a boundary condition that is a linear relation between the density and current of excited atoms at the surface of the discharge in the diffusion approximation.

Elastic and inelastic collisions and resonant exchange of excitation are two very important phenomena which have large influences on the emittance of the discharge. The effects of collisions are subsumed in the branching ratio for radiative decay of the resonance state. In practice, this number is very close to one as about two thirds of the photons get out of the discharge after typically hundreds of resonance-fluorescence processes. The importance of resonant exchange of excitation was

demonstrated in early experiments on nearly pure ^{198}Hg and an estimate of the cross section for this process was given.[4] We fit these two parameters to the shape of the emittance of the discharge as a function of temperature for natural Mercury. The numbers that we obtain from this fit are in good agreement with microscopic estimates.

Finally, the detailed structure of the ten component line must be included in the theory for a proper treatment of the effects of changes in the isotopic composition of the Mercury. Here the dominant effect is the overlap of neighboring lines. We use pure Doppler line shapes and have shown that the use of a schematic Voight profile does not alter our conclusions.

The ten excited state densities satisfy ten coupled integrodifferential equations that are modified versions of the Biberman-Holstein(BH) equation. These equations are to be solved subject to two point boundary conditions. Early studies of the BH equation concentrated on time dependent situations and the longest relaxation time - the "trapping time" - of the system. This time is only indirectly related to the emittance of the discharge in a time independent situation. Rather than following this traditional path, we have developed a theory for the emittance directly. We develop a variational principle for the emittance in Sec. 2. This principle by passes the problem of solving the equations for the excited state densities and reduces the problem of calculating a variational estimate of the emittance to quadrature after an appropriate choice of the ten trial excited-state and ten adjoint densities has been made.

In Sec. 3, we use our expression to evaluate the effects of changes in the isotopic concentration of the Mercury. Our choice of trial densities is motivated by a study of a simple one dimensional model which can be solved exactly and is discussed in an associated Lawrence Berkeley Laboratory Report.[5] We have also tested our method against an exact calculation for a model with a simplified line shape.[5] Some technical details of the full calculations are given in Appendix A. With ten components in the $^3P_1$ state of Mercury and our choice of trial densities, the resulting estimate of the emittance has forty linear variational parameters. They are determined for several temperatures about $40^\circ C$ for each isotopic mixture. The two sensitive parameters in the theory - the radiative decay probability for the $^3P_1$ state and the rate constant for collisional exchange of excitation - are obtained by fitting the temperature dependence of the emittance of natural Mercury. Three insensitive parameters are estimated from first principles. They are the total decay rate of the excited state and two boundary parameters. The first of the boundary parameters is the ratio of the current to the density of excited state Mercury at the surface. The second is the contribution of the current of excited state Mercury at the surface to the emittance. With these parameters fixed, there are no more adjustable parameters in the theory.

While there are seven naturally occurring isotopes of Mercury, we only consider cases in which a single pure isotope is added to or subtracted from natural Mercury as this is what is done in the laboratory and/or what would be done in practice at

least for the case of addition. We refer to this procedure as a change in the concentration of ^{A}Hg. We report results for A=196, 198, 199, 201, and 202 . Our results are in good agreement with experimentally observed results for A=196[6] and A=201[7] . We conclude that the theory is predictive for the additions of other isotopes. We show that additions of the isotopes with A=198, 199, 201, and 202 lead to changes of less than one percent and increases of less than 0.2% in the emittance. We also show that the small size of this effect is due to resonant exchange of excitation which leads to as much as a hundred-fold reduction of the effects of enrichment with these isotopes.

Background material and references to the literature can be found in Refs. 8-12. Specific models of the Hg-Ar discharge can be found in Refs. 13 and 14. We use the schematic model of Ref. 14 to represent the effects of changes in the Mercury density upon the electron density and temperature in the discharge in Sec. 3.

2. The variational principle.

In this section, we derive a variational principle for the radiant emittance of a low-pressure Mercury-Argon discharge. The basic equations that we use are an adaptation of those used in astrophysical theories of spectral line formation in stellar atmospheres.[6,7,8] This principle is a function of the total densities of each of the various Mercury isotopes, which are given as input, and a functional of the spatial distributions of

the atoms in the ten hyperfine components of the $^3P_1$ excited state, which are determined variationaly. It yields an estimate of the radiant emittance of the discharge and, with only minor modifications, the same principle can be used to provide estimates of the spectral line shape and/or the angular distribution of radiation leaving the surface of the discharge. However, here we will concentrate on the emittance as it is the quantity of prime importance in applications.

Our objective is the development of a theory that accounts for the effects of variations of the isotopic composition of the Mercury upon the emittance of the discharge. Changes in the isotopic composition redistribute the intensity over the isotope- and hyperfine-shifted components of the resonance line. The practical goal is the specification of the composition that maximizes the emittance by making the discharge more transparent without reducing the total source density. To this end, we make approximations that may not be appropriate in other contexts but which should not affect our conclusions which are based on differential rather than absolute results. These approximations are: (1) We assume that there is no time dependence and that the system has plane symmetry, i.e., a slab of thickness z_o. The qualitative effects that we seek to explain should not be affected by these assumptions since the longest relaxation time of the system is short compared to the typical period of 60 Hz and the mean-free-paths of particles and photons are short compared to the physical dimensions of the system. (2) We assume that the spectral line shapes are due to pure Doppler broadening.

This is a valid approximation for our situation in which the natural line width and pressure broadening effects are small compared to the Doppler width. A Voigt profile can be used for systems in which these effects may be important. We have tested our theory by using a schematic Voigt profile that has Lorentz wings grafted onto a Doppler core and found that these wings produce only small insignificant effects. (3) We assume that the photons are emitted and absorbed isotropically with the same line shape in both cases - complete redistribution in the lab frame. This is usually a good approximation in the core of a Doppler broadened line. The effects of partial redistribution on the wings of the line and the emittance will be considered in the future. (4) The Mercury atoms are assumed to be either in their $^1S_0$ ground state or their $^3P_0$ excited state - two level atoms. Losses are included by introducing a decay mode for the $^3P_1$ state in addition to radiative decay and electronic dexcitation. This mode represents the collisional destruction of the state to all final states which eventually end in the ground state but which do not contribute to the resonance radiation. The contribution of the $^1P_1$ excited state and its associated 180 nm resonance radiation will be considered in the future. (5) The electrons are assumed to have a density that varies cosinusoidally across the slab with a central density N_e and a vanishing density at the surface. They are assumed to have a Maxwell-Boltzmann energy distribution characterized by a temperature T_e. Typical values for these parameters are $N_e = 10^{12}$ cm^{-3} and $T_e = 10^4$ K. These numbers are put in by

hand and are not calculated from first principles. We do use a simple model of the discharge[14] to include the effects of changes in the Mercury density upon N_e and T_e in our applications. Calculations done with a parabolic spatial density distribution of electrons yield results that do not differ significantly from those obtained using a cosinusoidal distribution. (6) The Mercury ions and Argon atoms are passive elements in the theory and do not appear explicitly. The Argon, with a typical density of 10^{17} cm^{-3}, determines the diffusion constant for the Mercury. (7) The photons are described by the radiative transport equation which does not include photon polarization. The effects of photon polarization, magnetic fields, and alignment of the atomic states will be considered in the future. (8) We use the diffusion approximation to determine the spatial distributions of the various isotopes of Mercury in their ground and excited states. The diffusion terms in these equations are essential since they make a consistent treatment of important surface effects possible. However, the diffusion approximation is not strictly justifiable for the system under consideration and should be considered as an improvement upon existing theories that do not include diffusion. The more appropriate kinetic treatment of the Mercury will be treated in the future. (9) Surface effects are taken into account in two ways. First, we impose boundary conditions on the specific intensity of the radiation and atomic densities. And second, we allow for a contribution to the emittance from the current of excited atoms incident upon the surface. For the radiation field, the boundary

condition is that there be no incoming radiation at the surface. For the excited state atomic densities, we use a destroying boundary condition that all excited state atoms incident upon the surface are deexcited. In the diffusion approximation that we use, this leads to a linear combination of the density and the current vanishing at the surface. We estimate the coefficients in this condition from microscopic considerations and have shown that our results are not sensitive to their precise values. In the second effect, a contribution to the emittance can come from the deexcitation of the incident excited state atoms at the surface. This contribution is small compared to that of the photons but has a very different density, i.e., temperature dependence. It therefore has a significant effect on the determination of the parameters in the theory. (10) The equations are linearized in the excited state densities and stimulated emission of radiation is ignored. This can be justified on the basis of the smallness of the ratio of the excited-state to the ground-state densities which is smaller than the appropriate Boltzmann factor evaluated at T_e . We now use these assumptions to build a variational principle for the radiative flux at the surface of the discharge.

For time independent systems with planar geometry and surfaces perpendicular to the z-axis at $z = \pm z_0/2$, the radiative transport equation is

$$\mu \, \partial I_x(\zeta,\mu)/\partial\zeta = - \Lambda_x \, I_x(\zeta,\mu) + j_x(\zeta) \quad , \tag{2.1}$$

where $I_\nu(z,\mu) = (\tau k_{01} N_e)\ (2h\nu_o/\lambda_o^2)\ I_x(\zeta,\mu)$ is the specific intensity of the radiation field, $\mu = \cos\theta$ with θ the angle between the direction of propagation of the radiation and the z-axis, $\zeta = 2z/z_o$, $x = (\nu - \nu_o)/\Delta\nu$ with the Doppler line width given by $\Delta\nu = (2k_B T/Mc^2)^{1/2}\ \nu_o \cong 0.61$ GHz for $A = 200$ and $T = 315$ K , ν_o and λ_o are the frequency and wave length of the line center, N_e is the electron density at the center of the slab, k_{01} is the rate constant for excitation of the $^3P_1$ state, τ is the diffusion time, Λ_x is the absorption coefficient, and $j_x(\zeta)$ is the emission coefficient. The solution of (2.1) that satisfies the boundary condition of no entering radiation at the surfaces , is

$$I_x(\zeta,\mu) = \int_{\pm 1}^{\zeta} d\zeta'\ \exp[-\Lambda_x\ (\zeta - \zeta')/\mu]\ j_x(\zeta')/\mu\ ,\ \mu \lesseqgtr 0\ . \quad (2.2)$$

Equation (2.2) is completed by giving expressions for Λ_x and j_x . Using the two-level atom assumption, we have

$$\Lambda_x = \sum_i \Lambda_i\ \phi(x - x_i) \quad , \quad (2.3)$$

$$j_x(\zeta) = \frac{\Lambda_o}{3} \sum_i \eta_i^{1/2} \phi(x - x_i)\ f_i(\zeta) \quad , \quad (2.4)$$

with $\Lambda_i = \Lambda_o\ \eta_i$ and $\Lambda_o = \frac{3}{16\pi}(\lambda_o^2 z_o N_o)(A_{10}/\Delta\nu)$, where i labels the 10 isotope- and hyperfine-shifted components of the $^3P_1$ excited state of Mercury with the relationship between i and the atomic weight A_i , nuclear spin I_i , and total spin F_i given in Table 2.1 . In (2.2) and (2.3), $\nu_i = x_i \Delta\nu$ is the frequency of the line component, $\phi(x) = \pi^{-1/2}\exp(-x^2)$ is the

line shape, N_A is the ground state density of ^{A}Hg, $n_i(z) = N_o(\tau k_{01} N_e)\eta_i^{1/2} f_i(\zeta)$ is the density of Mercury atoms in component i of the $^3P_1$ excited state, where $\eta_i = w_i N_{A_i}/N_o$ with $N_o = 10^{14} cm^{-3}$ is a reference density, and A_{10} is the usual Einstein coefficient. The factor $w_i = (2F_i+1)/3(2I_i+1)$ is the ratio of the multiplicity of the hyperfine component to that of the excited state. The factor $\eta_i^{1/2}$ in the definition of f_i is chosen so as to lead to a self adjoint system of equations. The appearance of ϕ in both α_x and j_x reflects the assumption of complete redistribution.

We assume that the Mercury atoms diffuse through the Argon background with their internal states being changed by various collisional and radiative processes. The diffusion equations satisfied by the excited state densities are

$$[-\partial^2/\partial\zeta^2 + K_i(\zeta)]\, f_i(\zeta) = \eta_i^{1/2} \cos(\ell\zeta) \qquad (2.5)$$

$$+ \tau A_{10} \Sigma_j \int_{-1}^{1} d\zeta'\, M_{ij}(\zeta-\zeta')\, f_j(\zeta') + \Sigma_j L_{ij} f_j(\zeta) \quad .$$

The electron density has been taken to be

$$n_e(\zeta) = N_e \cos(\ell\zeta) \quad , \quad \ell = \pi/2 \; . \qquad (2.6)$$

The total decay rate in (2.5) is

$$K_i(\zeta) = \tau[A_{10} + A_\ell + k_{10}\, n_e(\zeta) + \Sigma_j\, \ell_{ij}\, N_o\, \eta_j] \quad , \qquad (2.7)$$

and the rate constants for resonant exchange of excitation are

$$L_{ij} = (\Lambda_i\Lambda_j)^{1/2}\, \tau\, \ell_{ij}\, N_o/\Lambda_o \quad .$$

The kernel of the integral is

$$M_{ij}(\zeta) = \frac{1}{2} (\Lambda_i \Lambda_j)^{1/2} \int_{-\infty}^{\infty} dx\ \phi(x - x_i)\ \phi(x - x_j)\ E_1(\Lambda_x |\zeta|) \ , \tag{2.8}$$

where E_1 is an exponential integral[13]

$$E_n(z) = \int_0^1 d\mu\ \mu^{n-2}\ e^{-z/\mu} \ . \tag{2.9}$$

Note that $M_{ij}(\zeta - \zeta')$ is symmetric in both i and j and ζ and ζ'. This plus the symmetry of L_{ij}, makes (2.5) a self adjoint system of equations for the f_i. The two terms on the left-hand-side represent the decay of the density of atoms in the state i at the point ζ due to diffusion and deexcitation respectively. The three source terms on the right-hand-side represent the increase in this density due to electronic, radiative, and resonant excitation of the ground state respectively.

The f_i are even functions of ζ that satisfy the appropriate boundary conditions at $\zeta = \pm 1$. In our model, the surface deexcites all excited state atoms incident upon it. In the diffusion approximation and in our dimensionless units, this implies

$$[b\ \partial f_i/\partial \zeta + f_i]_{\zeta = \pm 1} = 0 \ , \tag{2.10}$$

where $b \cong 2D(2\pi M/kT)^{1/2}/z_o \cong 1.33 \times 10^{-3}$. This estimate comes from assuming that the excited state atoms are in a Maxwell-Boltzmann distribution with temperature T and that all atoms incident upon the surface are deexcited. The numerical estimate comes from taking the Mercury-Argon collision rate to be

$\nu_c \cong 10^7$ sec.$^{-1}$. While the numerical value of b is uncertain, we have shown that that our results are not sensitive to its value.

We assume that the radiant emittance of the discharge is the sum of photon and atom contributions, $J = J_{phot} + J_{atom}$. The photon part is the flux of energy in photons

$$J_{phot} = 2\pi \int_o^\infty d\nu \int_o^1 d\mu\ \mu\ I_\nu(z_o/2,\mu) \qquad (2.11)$$

$$= J_o \sum_i \eta_i^{1/2} \int_{-\infty}^{\infty} dx\ \phi(x-x_i) \int_{-1}^{1} d\zeta\ E_2[\Lambda_x(1-\zeta)]\ f_i(\zeta) \quad ,$$

where $J_o = (2\pi/3)(\tau k_{01} N_e)\Lambda_o(2h\nu_o/\lambda_o^2)\Delta\nu$. The atom part of the emittance is the energy deposited on the surface by the deexcitation of the incident current of excited atoms. We write it as

$$J_{atom} = J_o\ s \sum_i \eta_i^{1/2}\ [\partial f_i/\partial\zeta]_{\zeta=1} \quad , \qquad (2.12)$$

where s is a measure of the relative importance of this surface contribution. If all the energy deposited by the atoms is utilized by the phosphor as if it were UV radiation, then we estimate $s \cong 5.21\times10^{-5}$. Thus, the surface contribution is small but it does have an influence on the determination of the parameters of the theory. While the numerical value of s is very uncertain, our results are insensitive to its value if the other parameters are chosen to fit the data on natural Mercury.

We construct a variational principle for J by defining the functional

$$J_v = \sum_i \eta_i^{1/2} \Big[s\, [\partial f_i/\partial\zeta]_{\zeta=1} \tag{2.13}$$

$$+ \int_{-\infty}^{\infty} dx\ \phi(x-x_i) \int_{-1}^{1} d\zeta\ \frac{1}{2} \{E_2[\Lambda_x(1-\zeta)] + E_2[\Lambda_x(1+\zeta)]\}\ f_i(\zeta) \Big]$$

$$+ \sum_i \int_{-1}^{1} d\zeta\ F_i(\zeta) \Big[\eta_i^{1/2} \cos(\ell\zeta) - [-\partial^2/\partial\zeta^2 + K_i(\zeta)]\ f_i(\zeta)$$

$$+ \sum_j \Big[\int_{-1}^{1} d\zeta'\ M_{ij}(\zeta-\zeta')\ f_j(\zeta') + L_{ij}\ f_j(\zeta) \Big] \Big] \ ,$$

where f_i and F_i are now interpreted as trial functions. The first term in (2.13) comes from the surface contribution and the second term comes from symmetrizing the kernel in (2.11). The remaining terms come from the introduction of the set of adjoint functions $F_i(\zeta)$ that are used to impose the conditions that the $f_i(\zeta)$ satisfy (2.5) in the form $\delta J_v/\delta F_i(\zeta) = 0$. Equations for the F_i are obtained from $\delta J_v/\delta f_i(\zeta) = 0$ plus the boundary conditions (2.10) with f_i replaced by F_i . These equations are the same as (2.5) but with the inhomogeneous terms replaced by

$$\frac{1}{2}\ \eta_i^{1/2} \int_{-\infty}^{\infty} dx\ \phi(x-x_i)\ \{\ E_2[\Lambda_x(1-\zeta)] + E_2[\Lambda_x(1+\zeta)]\ \}\ . \tag{2.14}$$

Thus, since $J_v = J/J_o$ when the F_i or f_i satisfy their respective equations and J_v is stationary at that point, it provides a variational estimate of J/J_o when it is evaluated using suitable trial functions.

We choose trial functions suggested by the solution of a

simplified one-dimensional model[5]

$$f_i(\zeta) = \sum_{\alpha=1,2} f_{i\alpha}\, g_\alpha(\zeta) \quad , \tag{2.15}$$
$$F_i(\zeta) = \sum_{\alpha=1,2} F_{i\alpha}\, g_\alpha(\zeta) \quad ,$$

where

$$g_1(\zeta) = b\ell + \cos(\ell\zeta) \quad , \tag{2.16}$$
$$g_2(\zeta) = bk\tanh(k) + 1 - \cosh(k\zeta)/\cosh(k) \quad .$$

These functions satisfy the boundary condition (2.10). The constants $f_{i\alpha}$ and $F_{i\alpha}$, $i=1,\cdots,10$ and $\alpha=1,2$ are forty linear variational parameters. The parameter k can be taken as a nonlinear variational parameter when $b = s = 0$. In this case, J_v has a very weak maximum as a function of k when the parameters of the theory are chosen as in Sec. 3. However, when b and/or s are different from zero, the derivative terms dominate the expression for J_v when k is large and it does not have a stationary value as a function of k. In this case, we use a the value suggested by the $b=s=0$ calculation and we have shown that our results are not sensitive to this choice of k.

Substitution of (2.21) into (2.19) yields the expression

$$J_v = \Lambda_o^{-1/2} \sum_{i\alpha} [A_{i\alpha} f_{i\alpha} + B_{i\alpha} F_{i\alpha}]$$

$$- K_o \sum_{i\alpha,j\beta} F_{i\alpha}\, C_{i\alpha,j\beta}\, f_{j\beta} \quad , \tag{2.17}$$

where

$$A_{i\alpha} = \Lambda_i^{1/2} \int_{-\infty}^{\infty} dx\ \phi(x-x_i) \int_{-1}^{1} d\zeta\ E_2[\Lambda_x(1-\zeta)]\ g_\alpha(\zeta) \quad , \tag{2.18}$$

$$B_{i\alpha} = \Lambda_i^{1/2} \int_{-1}^{1} d\zeta \cos(\ell\zeta)\, g_\alpha(\zeta) \quad , \tag{2.19}$$

$$C_{i\alpha,j\beta} = \int_{-1}^{1} d\zeta\, g_\alpha(\zeta)\, [(K_1 - (\partial^2/\partial\zeta^2)/K_o)\, \delta_{ij} - L'_{ij}]\, g_\beta(\zeta) - a' \int_{-1}^{1} d\zeta\, d\zeta'\, g_\alpha(\zeta)\, M_{ij}(\zeta - \zeta')\, g_\beta(\zeta') \quad , \tag{2.20}$$

and where we have simplified K_i of (2.7) by defining

$$K_o = \tau(A_{10} + A_\ell) \quad ,$$

$$K_1 = 1 + (\tau\Sigma_j\, \ell_{ij}\, N_o\, \eta_j)/K_o = 1 + \tau\ell_o N_{Hg}/K_o \quad ,$$

and neglecting the spatial dependence of the small electronic deexcitation term. We have also defined $L'_{ij} = L_{ij}/K_o$ and $a' = a/K_o$. The results of doing all but the frequency integrations in (2.18) - (2.20) are given in Appendix A for the choice of trial function (2.16). The frequency integrations must be done numerically. Requiring J_v to be stationary with respect to the linear parameters $f_{i\alpha}$ and $F_{i\alpha}$ yields

$$J_v = \frac{1}{\Lambda_o K_o} \sum_{i\alpha,j\beta} A_{i\alpha}\, C^{-1}_{i\alpha,j\beta}\, B_{j\beta} \quad . \tag{2.21}$$

This expression for the emittance is the basis for our study of the effects of isotopicly enhanced mixtures on the emittance given in the next section.

3. Isotopic mixtures.

Calculations of the effects of changes in the isotopic concentrations of the Mercury on the radiant emittance of the discharge must proceed in two steps. First, the parameters of

the theory must be fixed and then the isotopic concentrations can be varied. The parameters fall into three classes. In the first class are the parameters that have a large effect upon the emittance : a' - the branching ratio for radiative decay of the $^3P_1$ state and ℓ_o - the rate constant for resonant exchange of excitation. These two parameters are fitted to the temperature dependence of the emittance of natural Mercury, that is, the location of the temperature at which the emittance is a maximum which we take to be 40^oC and the rise of the emittance over the interval from 20^oC to 40^oC which we take to be 40% . The members of second class of parameters have only a weak effect upon the emittance and are given estimated values. They are: K_o - the diffusion time times the total decay rate for the $^3P_1$ state which we take to be $K_o \cong 10^5$ (based upon a diffusion time $\tau \cong 0.01$ sec. and a decay rate that is dominated by radiative decay $A_{10} \cong 10^7$ sec.$^{-1}$) and the boundary condition and surface contribution constants which have already been discussed $b \cong 1.33\times10^{-3}$ and $s \cong 5.21\times10^{-5}$. The only member of the third class is the nonlinear parameter k in the trial functions. This can be determined variationally for $b = s = 0$ and takes on values near but less than $K_o^{1/2}$ as expected from the results reported Ref. 5. When b and/or s are different from zero, J_v no longer has a stationary point with respect to k . We set $k = 100$ in our calculations and have shown that our results are not sensitive to this choice.

We can estimate the values of a' and ℓ_o from the following qualitative considerations. We first have, by

definition, $a' \leq 1$. A lower bound can be obtained from the empirical fact that about two thirds of the photons reach the surface after about one hundred resonance fluorescence processes which requires $a' > 0.996$. We obtain $a' = 0.99684$ from our fit to natural Mercury. For ℓ_o , we use $\ell_o \cong \tau<\sigma v>N_o/K_o\Lambda_o$ and $\sigma \cong 10^{-13}cm.^2$ to estimate $\ell_o \cong 10^{-3} - 10^{-4}$. Our fitted value is $\ell_o = 9.8\times10^{-5}$. Thus our fitted values of the parameters are quite reasonable. There are no further fitted parameters in the calculations for isotopicaly enriched Mercury.

In all of the isotopic mixtures that we discuss, we modify concentrations by adding or subtracting pure amounts of the isotope to be modified as this is how it is done in the laboratory at least for additions. We then calculate the emittance at 2K intervals from 307K to 319K using (2.21). Then, for each isotopic mixture, we look for the maximum value of the emittance as a function of temperature. We present in the tables the change in this maximum emittance from that of natural Mercury in percent. This is done for changes in the Mercury-196 concentration in Table 3.1 and for Mercury- 198, 199, 201, and 202 concentrations in Table 3.2. In both of these tables, we use the natural concentration as the unit of concentration for each isotope. The small numbers in Table 3.2, which are the difference between two large numbers, should be treated with caution and are only meant to suggest trends.

The effects of changes in Mercury density upon the electron density N_e and temperature T_e are included in this calculation through the schematic model of the discharge of

Ref. 14. This leads an overall multiplicative temperature dependant correction of the form $N_e(T)\exp(-E_1/kT_e(T))$ which decreases strongly with increasing temperature due to the increasing density of the Mercury. This has a large effect upon the determination of a' and ℓ_o and through them on the results presented in the Tables.

Our results for increases in the ^{196}Hg concentration are given in Table 3.1. They imply a maximum increase in the emittance of 5.4% at a concentration of 11.6% or 59 times natural. This is in good agreement with published experimental results[6] and gives strong support for our theory.

Our results for Mercury-198, 199, 201, and 202 are given in Table 3.2. The changes in the emittance are all very small for changes in the concentrations between 0.2 to 2.0 times natural. The results for the increases in the concentration of ^{201}Hg are in agreement with unpublished experimental results[5]. We conclude that there is no practical gain from changing the concentrations of these isotopes. We have also spot checked changes in the ^{200}Hg and ^{204}Hg with similar insignificant results. The important role played by resonant exchange of excitation in obtaining these results should be emphasized. If we consider the artificial problem with $\ell_o = 0$, Then the ^{196}Hg results remain about the same but the effects of enhancing the other isotopes are about a hundredfold larger.

Appendix A. Integrals.

In this appendix, we give explicit expressions for the

arrays $A_{i\alpha}$, $B_{i\alpha}$, and $C_{i\alpha,j\beta}$ of Eqs. (2.18) - (2.20) for the choice of trial functions (2.15). The spatial and angular integrations are done explicitly and the results are given in terms of frequency integrals which must be done numerically.

We rewrite (2.18) for $A_{i\alpha}$ as

$$A_{i\alpha} = \Lambda_i^{1/2} \int_{-\infty}^{\infty} dx\ \phi(x - x_i)\ a_\alpha(\Lambda_x) \quad , \tag{A.1}$$

where

$$a_\alpha(\Lambda) = \int_0^1 d\mu \int_{-1}^{1} d\zeta\ e^{-\Lambda(1-\zeta)/\mu}\ g_\alpha(\zeta) \tag{A.2}$$

and g_α is given by (2.15). The ζ-integration in (A.2) is straightforward and the μ-integration can be done using techniques described by Chandrasekhar[6] with the results , for α=1,

$$a_1(\Lambda) = b\ell\ [1 - 2E_3]/2\Lambda + \{1 - \Lambda[\tan^{-1}(\ell/\Lambda) + E_1']/\ell + E_2\} \tag{A.3}$$

where $E_n = E_n(2\Lambda)$ and in this Appendix we use the notation $E_1(2\Lambda+i\pi) = E_1' + i\ E_1''$ and $E_n(z)$ is defined in (2.9).

For α=2 , we have

$$a_2(\Lambda) = (1 + bkT)[1 - 2E_3]/2\Lambda - T[1 + E_2]/k - \Lambda\ E_1/k^2 + \Lambda\{(1 + T)[\ln(1 + k/\Lambda) + E_1(2\Lambda + 2k)] + (1 - T)[\ln(|1 - k/\Lambda|) - Ei(2k - 2\Lambda)]\}/2k^2 \quad , \tag{A.4}$$

where $T = \tanh(k)$ and the exponential integral[13] is given by

$$Ei(u) = -\int_{-u}^{\infty} dt\ e^{-t}/t \quad , \ u > 0 \ ,$$

where the principal value is taken and $Ei(-u) = -E_1(u)$.

The integrations for the $B_{i\alpha}$ are all elementary with

$$B_{i1} = \Lambda_i^{1/2} \ (1 + 2b) \quad ,$$

$$B_{i2} = 2\Lambda_i^{1/2} \ [k^2/(k^2 + \ell^2) + bkT \ ] \quad . \tag{A.5}$$

For the matrix C , we write

$$C_{i\alpha,j\beta} = \delta_{ij} \ C^{(0)}_{\alpha\beta} - L_{ij}' \ C^{(1)}_{\alpha\beta} - a' \ C^{(2)}_{i\alpha,j\beta} \quad , \tag{A.6}$$

where

$$C^{(0)}_{\alpha\beta} = \int_{-1}^{1} d\zeta \ g_\alpha(\zeta) \ [K' - \frac{1}{K_o} \frac{\partial^2}{\partial\zeta^2}] \ g_\beta(\zeta) \quad , \tag{A.7}$$

$$C^{(1)}_{\alpha\beta} = \int_{-1}^{1} d\zeta \ g_\alpha(\zeta) \ g_\beta(\zeta) \quad , \tag{A.8}$$

and

$$C^{(2)}_{i\alpha,j\beta} = (\Lambda_i\Lambda_j)^{1/2} \int_{-\infty}^{\infty} \frac{dx}{\sqrt{\pi}} \ \phi(x - x_i) \ \phi(x - x_j) \ c_{\alpha\beta}(\Lambda_x) \tag{A.9}$$

with

$$c_{\alpha\beta}(\Lambda) = \int_0^1 \frac{d\mu}{\mu} \int_{-1}^{1} d\zeta \ d\zeta' \ g_\alpha(\zeta) \ \exp[-\Lambda|\zeta - \zeta'|/\mu] \ g_\beta(\zeta') \tag{A.10}$$

All integrations except that over frequency in (A.10) can be done explicitly with the results

$$C^{(0)}_{1,1} = [1 + 4b + 2(bl)^2] \ K' + \ell^2(1 + 2b) \quad , \tag{A.11}$$

$$\begin{aligned} C^{(0)}_{1,2} &= 2\{k^2/\ell(k^2+\ell^2) + b[\ell + (k/\ell - \ell/k)T] + b^2\ell kT \ \}K' \\ &\quad + 2\ell(k^2/(k^2+\ell^2) + bT/k) \ , \\ &= C^{(0)}_{2,1} \quad , \end{aligned}$$

$$C^{(0)}_{2,2} = [(3+4bkT)(1 - T/k) - T^2 + 2(bkT)^2]K' + kT - k^2 + (1 + 4b)k^2T^2,$$

$$C^{(1)}_{1,1} = 1 + 4b + 2(bl)^2 \quad ,$$

$$C^{(1)}_{1,2} = 2\{k^2/\ell(k^2+\ell^2) + b[\ell + (k/\ell - \ell/k)T] + b^2\ell kT\} \quad ,$$

$$= C^{(1)}_{2,1} \quad ,$$

$$C^{(1)}_{2,2} = (3+4bkT)(1 - T/k) - T^2 + 2(bkT)^2 \quad ,$$

$$c_{1,1}(\Lambda) = (1 + 2b)[\tan^{-1}(\ell/\Lambda) + E_1'']/\ell - (1+e^{-2\Lambda})/2(\Lambda^2+\ell^2) + 2b[1 - E_2]/\Lambda + 2[\ln(1 + \ell^2/\Lambda^2)/2 + E_1 + E_1']/\ell^2 + (b\ell)^2[2 - (1 - 2E_3)/2\Lambda]/\Lambda,$$

$$c_{1,2}(\Lambda) = [1/\ell + b(k/\ell - \ell/k)T][1 - E_2]/\Lambda - (T/\ell k - b\ell/k^2)E_1 + 2bkT\tan^{-1}(\ell/k) + b\ell(1 + bkT)[2 - (1 - 2E_3)/2\Lambda]/\Lambda + [k^2/(k^2+\ell^2) - bkT][\tan^{-1}(\ell/k) + E_1'']/\ell^2 - kT[\ln(1 + \ell^2/\Lambda^2)/2 + E_1']/\ell(k^2+\ell^2) - \ell\{(1+T)[1/(k^2+\ell^2) + b/k][\ln(1 + k/\Lambda) + E_1(2k+2\Lambda)] - (1-T)[1/(k^2+\ell^2) - b/k][\ln(|1 - k/\Lambda|) - Ei(2k-2\Lambda)]\}/2k$$

$$= c_{2,1}(\Lambda) \quad ,$$

$$
\begin{aligned}
c_{2,2}(\Lambda) = {} & (1+bkT)^2\,[2 - (1 - 2E_3)/2\Lambda]/\Lambda \\
& - 2T(1+bkT)(1 - E_2)/k\Lambda + (2+T^2+2bkT)E_1/k^2 \\
& + (1+T)[1- T- (2- T+2bkT)/k][\ln(1 + k/\Lambda) + E_1(2k+2\Lambda)]/2k \\
& - (1- T)[1+T+(2+T+2bkT)/k][\ln(|1 - k/\Lambda|) - Ei(2k- 2\Lambda)]/2k \\
& + (1- T^2)\{[1- e^{-2(\Lambda+k)}]/(\Lambda+k) - [1- e^{-2(\Lambda- k)}]/(\Lambda- k)\}/4k.
\end{aligned}
$$

While somewhat messy, the above expressions for a_α and $c_{\alpha\beta}$ can be substituted into (A.1) and (A.9) and the frequency integrations done by numerical methods. The resulting arrays $A_{i\alpha}$, $B_{j\beta}$, and $C_{i\alpha,j\beta}$ can then be substituted into (2.21) to give a variational estimate of the emittance.

Table 2.1. Components of the $^3P_1$ state of Mercury. Atomic weight A_i, Nuclear spin I_i, total spin F_i, and frequency displacement from the A = 200 line $\nu_i - \nu_9$.

i	A_i	I_i	F_i	$\nu_i - \nu_9$(GHz)
1	199	1/2	1/2	-11.25
2	204	0	1	-10.51
3	201	3/2	5/2	-9.86
4	201	3/2	3/2	4.14
5	198	0	1	4.81
6	199	1/2	3/2	11.49
7	201	3/2	1/2	11.68
8	202	0	1	-5.30
9	200	0	1	0.00
10	196	0	1	8.91

Table 3.1. Percentage change of the emittance for increased concentration of ^{196}Hg . The concentration x is given in units of the natural concentration. The parameters are: $K=10^5$, $a'=0.99684$, $\ell_o=9.8\times10^{-5}$, $b=1.33\times10^{-3}$, $s=5.21\times10^{-5}$, and $k=100$.

x	2	4	8	16	32	64	128
Change	0.61	1.51	2.90	4.35	5.21	5.37	5.11

Table 3.2. Percentage change of the emittance for changes in the concentrations of isotopes with A = 198, 199, 201, and 202. The concentrations x are given in units of the natural concentrations and the parameters are those given in Table 3.1.

x\A	198	199	201	202
0.2	-0.53	-0.65	-0.03	-0.68
0.4	-0.28	-0.10	0.26	0.00
0.6	-0.21	0.03	0.13	0.09
0.8	-0.09	0.06	0.13	0.07
1.2	0.07	-0.07	-0.12	-0.10
1.4	0.12	-0.10	-0.07	-0.23
1.6	0.07	-0.13	-0.16	-0.40
1.8	0.06	-0.11	-0.04	-0.57
2.0	0.14	-0.19	-0.11	-0.84

References

1. L. M. Biberman, Dokl. Akad. Nauk. 27, 920 (1940); Zh. Eksp. Teor. Fiz. 17, 416 (1947) [Trans. Sov. Phys. JETP 19, 584 (1949)].

2. T. Holstein, Phys. Rev. 72, 1212 (1947); 83, 1159 (1951).

3. R. W. Richardson and S. M. Berman, J. Quant. Spectrosc. Radiat. Transfer 37, 471 (1987).

4. T. Holstein, D. Alpert, and A. O. McCoubrey, Phys. Rev. 85, 985 (1952).

5. R. W. Richardson and S. M. Berman Lawrence Berkeley Laboratory Report LBID 1759.

6. J. Maya, et al, Science 226, 435 (1984).

7. D. Hollister, Private communication.

8. S. Chandrasekhar, Radiative Transfer, (Oxford University Press, 1950; Reprinted by Dover Publications, Inc. 1960 New York.)

9. D. Mihalas, Stellar Atmospheres, 2nd. Ed., (Freeman, San Francisco, 1978).

10. J. Oxenius, Kinetic Theory of Particles and Photons, (Springer-Verlag, Berlin 1986).

11. L. M. Biberman, et al, Kinetics of Nonequilibrium Low Temperature Plasmas, (Consultants Bureau, New York 1987).

12. A. E. Bulyshev, et al, Usp. Fiz Nauk. 156, 153 (1988); [Trans. Sov. Phys. Usp. 31, 865 (1989)].

13. J. F. Waymouth and F. Bitter, J. Appl. Phys. 27, 122 (1956).

14. W. L. Lama, et al, Appl. Opt. 21, 1801 (1982).

15. M. Abramowitz and I. A. Stegun, Eds., Handbook of Mathematical Functions, (Dover Publications, Inc., New York 1972) Chapt. 5.

LAWRENCE BERKELEY LABORATORY
UNIVERSITY OF CALIFORNIA
TECHNICAL INFORMATION DEPARTMENT
BERKELEY, CALIFORNIA 94720